JNS

CLINICAL ARTICLE

J Neurosurg 136:1694–1704, 2022

Aneurysm presence at the anterior communicating artery bifurcation is associated with caliber tapering of the A_1 segment

Alexandra Lauric, PhD, Luke Silveira, MD, Emal Lesha, MD, Jeffrey M. Breton, MD, and Adel M. Malek, MD, PhD

Department of Neurosurgery, Tufts Medical Center and Tufts University School of Medicine, Boston, Massachusetts

OBJECTIVE Vessel tapering results in blood flow acceleration at downstream bifurcations (firehose nozzle effect), induces hemodynamics predisposing to aneurysm initiation, and has been associated with middle cerebral artery (MCA) aneurysm presence and rupture status. The authors sought to determine if vessel caliber tapering is a generalizable predisposing factor by evaluating upstream A_1 segment profiles in association with aneurysm presence in the anterior communicating artery (ACoA) complex, the most prevalent cerebral aneurysm location associated with a high rupture risk.

METHODS Three-dimensional rotational angiographic studies were analyzed for 68 patients with ACoA aneurysms, 37 nonaneurysmal contralaterals, and 53 healthy bilateral controls (211 samples total). A_1 segments were determined to be dominant, codominant, or nondominant based on flow and size. Equidistant cross-sectional orthogonal cuts were generated along the A_1 centerline, and cross-sectional area (CSA) was evaluated proximally and distally, using intensity-invariant edge detection filtering. The relative tapering of the A_1 segment was evaluated as the tapering ratio (distal/proximal CSA). Computational fluid dynamics was simulated on ACoA parametric models with and without tapering.

RESULTS Aneurysms occurred predominantly on dominant (79%) and codominant (17%) A_1 segments. A_1 segments leading to unruptured ACoA aneurysms had significantly greater tapering compared to nonaneurysmal contralaterals (0.69 ± 0.13 vs 0.80 ± 0.17, $p = 0.001$) and healthy controls (0.69 ± 0.13 vs 0.83 ± 0.16, $p < 0.001$), regardless of dominance labeling. There was no statistically significant difference in tapering values between contralateral A_1 and healthy A_1 controls (0.80 ± 0.17 vs 0.83 ± 0.16, $p = 0.56$). Hemodynamically, A_1 segment tapering induces high focal pressure, high wall shear stress, and high velocity at the ACoA bifurcation.

CONCLUSIONS Aneurysmal, but not contralateral or healthy control, A_1 segments demonstrated significant progressive vascular tapering, which is associated with aneurysmogenic hemodynamic conditions at the ACoA complex. Demonstration of the upstream tapering effect in the communicating ACoA segment is consistent with its prior detection in the noncommunicating MCA bifurcation, which together form more than 50% of intracranial aneurysms. The mechanistic characterization of this upstream vascular tapering phenomenon is warranted to understand its clinical relevance and devise potential therapeutic strategies.

https://thejns.org/doi/abs/10.3171/2021.5.JNS204389

KEYWORDS intracranial aneurysms; ACoA aneurysms; vessel tapering; aneurysm presence; vascular disorders

Aneurysms located at the anterior communicating artery (ACoA) account for 30%–37% of all intracranial aneurysms and are frequently associated with subarachnoid hemorrhage (SAH).[1] Cerebral aneurysm size is clinically correlated with rupture risk,[2] although ACoA aneurysms are known to hemorrhage at relatively small sizes[1] compared to aneurysms at other locations. Because of their many anatomical variations and communicating characteristics, ACoA aneurysms can be challenging to treat by either microsurgical or endovascular means.[1] The greater prevalence of ACoA aneurysms compared to those at other locations, and their high rupture rate, make the study of this location and the understanding of the underlying mechanisms for aneurysm origination and progression of particular clinical importance.

The rationale for this study focused on ACoA aneurysms is based on recent findings in middle cerebral artery (MCA) aneurysms,[3] which showed that M_1 segments lead-

ABBREVIATIONS 3DRA = three-dimensional catheter-based cerebral angiogram; ACA = anterior cerebral artery; ACoA = anterior communicating artery; CFD = computational fluid dynamics; CSA = cross-sectional area; MCA = middle cerebral artery; SAH = subarachnoid hemorrhage; WSS = wall shear stress.

SUBMITTED December 21, 2020. **ACCEPTED** May 17, 2021.

INCLUDE WHEN CITING Published online October 15, 2021; DOI: 10.3171/2021.5.JNS204389.

©AANS 2022, except where prohibited by US copyright law

Brought to you by Tufts University | Unauthenticated | Downloaded 11/04/25 02:23 PM UTC

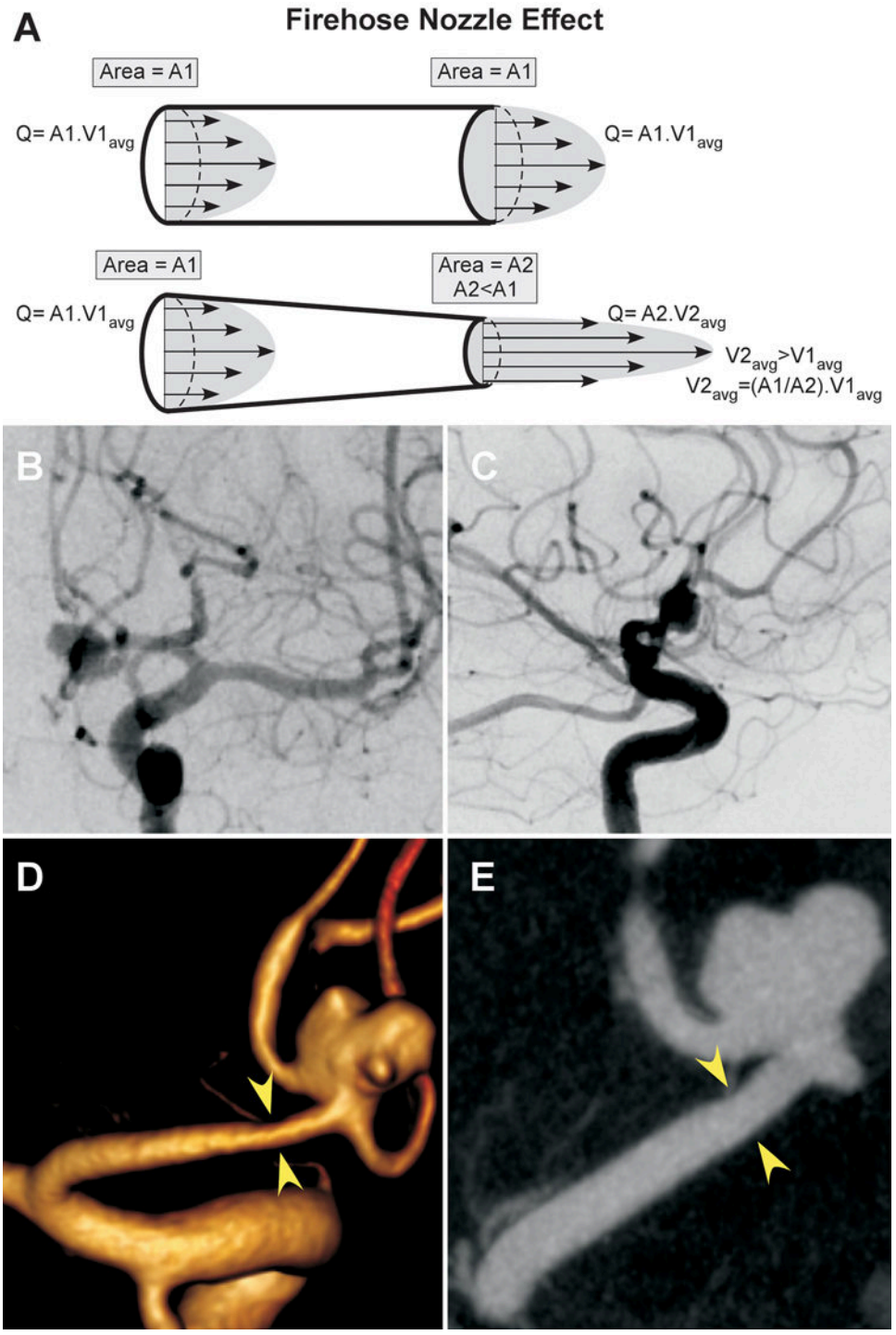


FIG. 1. A: Schematic representation of vessel tapering akin to a "firehose nozzle effect." Assuming a parabolic velocity profile, this phenomenon leads to flow acceleration and higher velocity toward the bifurcation apex. Q = volume flow; V = flow velocity. **B and C:** Anteroposterior (B) and lateral (C) projection digital subtraction angiograms of a patient with an ACoA aneurysm. **D:** Three-dimensional virtual rendering of the rotational angiographic data set showing tapering (*arrows*) of the left A_1 segment of the ACA proximal to the aneurysm. **E:** Multiplanar reconstruction of the same data set showing corresponding focal stenosis (*arrows*). Figure is available in color online only.

ing to MCA aneurysms demonstrated progressive distal tapering, which was not observed in corresponding contralateral studies nor in healthy controls. Particularly in healthy patients, M_1 segments showed no vessel tapering. This statistically significant upstream vessel narrowing, similar to the tapering seen in firehose nozzles (Fig. 1), was shown to lead to flow acceleration and higher velocity toward the bifurcation apex (in accordance with conserva-

Brought to you by Tufts University | Unauthenticated | Downloaded 11/04/25 02:23 PM UTC

tion of mass and the incompressible nature of blood flow), and to result in increased wall shear stress (WSS) and related spatial gradients,[3,4] thus creating favorable hemodynamic conditions for aneurysm initiation and progression.[5]

In this study we investigate if the vessel tapering phenomenon previously demonstrated in MCA aneurysms—termed the "firehose nozzle effect"—is also present in the case of ACoA aneurysms, and thus a generalized phenomenon. The analysis is focused on the A_1 segment of the anterior cerebral artery (ACA) and is performed bilaterally in patients with unruptured ACoA aneurysms, as well as in healthy controls.

Methods

Patient Selection

Consecutive high-resolution 3D angiographic data of patients undergoing cerebral angiography were reviewed for this study from a prospectively maintained database. The patient selection flow diagram is available as Supplementary Fig. 1. All angiographic investigations were performed for medical reasons, prior and unrelated to this study. All angiographic studies of patients harboring ACoA aneurysms and having imaging of sufficient quality to permit accurate segmentation and morphological analysis were included in the study. When available, bilateral angiographic data of the contralateral nonaneurysmal side were also included. In addition, angiographic data from patients without cerebral aneurysms, undergoing workup for other medical reasons (Supplementary Table 1), were considered for analysis if bilateral angiography of sufficient quality was available. Very young control patients (age < 20 years) were excluded from analysis to ensure that aneurysmal and control groups were age matched. All angiographic data within this set were obtained on an emergency basis and prior to vasospasm onset.

This research was approved by Tufts Health Sciences Campus IRB. Patient consent was waived because of the retrospective nature of the study not impacting patient clinical care.

Cerebral Angiography and Data Processing

Three-dimensional catheter-based cerebral angiograms (3DRAs) were obtained using a Siemens Artis calibrated biplane system, with volume reconstruction using Siemens Leonardo clinical software package, to yield a 3D volumetric data set. Volumetric data sets, including aneurysm and parent vessel, were analyzed using Amira (version 5.3) and MATLAB R2017 (MathWorks).

A_1 Segment Dominance

Angiographic filling of the A_1 segment was evaluated for all data sets. The A_1 segments were evaluated as the dominant, nondominant, and codominant segments based on size and angiographic presentation. The aneurysmal A_1 segment (left/right) was selected as the side that provided a complete filling of the aneurysm on the corresponding angiographic images. Bilateral volumes were visualized and examined simultaneously using Amira (Figs. 2 and 3A), a software platform for 3D data visualization, processing, and analysis.

Morphological Feature Extraction

The skeleton (centerline) of the A_1 segment of the ACA was generated using Amira and exported to MATLAB to generate equidistant orthogonal cross-sections along the entire A_1 segment (Fig. 3B). Edge detection filtering was applied to all cross-sections, which yields intensity and windowing invariant results;[6] this has been previously shown to enable detection of very small diameter changes consistently without windowing artifacts. The cross-sectional area (CSA) of the A_1 segment was evaluated from the edge detection results (Fig. 3C). To ensure a consistent evaluation of area measurements, proximal and distal cross-sections were considered at 1, 1.5, and 2 mm from the ICA and ACoA bifurcations, respectively. The following measurements were used for analysis: 1) the proximal CSA of the A_1 segment, measured 1 mm from the ICA bifurcation; 2) the distal CSA, as the area of the most distal plane cut closest to the MCA bifurcation measured 1 mm from the ACoA bifurcation; 3) the tapering of the A_1 segment (tapering ratio) defined as distal CSA/proximal CSA, as the ratio of the distal CSA to the proximal CSA; and 4) the length of the A_1 segment (A_1 length).

Statistical Analysis

JMP statistical software (version 14.0, SAS Institute) was used to evaluate the performance of all parameters in discriminating between aneurysmal and control ACoA data sets. Statistical significance was assumed for p values < 0.05. All variables were tested independently using the Student t-test. Bilateral A_1 analysis within the same patient was performed using matched-pair analysis.

Parametric Geometrical Models

Parametric models of the anterior communicating complex (bilateral ACA including the ACoA) were created to evaluate the effect of A_1 segment tapering on the ACoA bifurcation hemodynamic environment. The models were created using SpaceClaim (Ansys 19.2, Ansys Inc.).

The A_1 segment of the ACA was modeled at 30° inclination from the vertical axis, with a diameter of 2 mm and a length of 40 mm, followed by a vertical A_2 segment with a diameter of 2 mm and a length of 30 mm. Bilateral vessels were modeled symmetrically and connected with an ACoA segment with a diameter of 1 mm and a length of 2.5 mm (Fig. 4A). A second model was created by distal tapering of the A_1 segments. One of the segments was tapered from 2 mm to 1.25 mm, and the second from 2 mm to 1.75 mm (Fig. 4A).

Computational Fluid Dynamics

The two models were used to create dynamic tetrahedral and prism meshes with boundary layer enhancement using Workbench (version 19.2, Ansys Inc.). Computational fluid dynamics (CFD) simulations were performed using Ansys Fluent (version 19.2, Ansys Inc.), by modeling steady-state laminar flow with a Carreau non-Newtonian profile to better approximate the viscosity and flow of blood.[7] To account for variability in the size, shape, and length of the parent vessel, flow scaling factors were determined for the nontapered model to ensure ideal parent

Brought to you by Tufts University | Unauthenticated | Downloaded 11/04/25 02:23 PM UTC

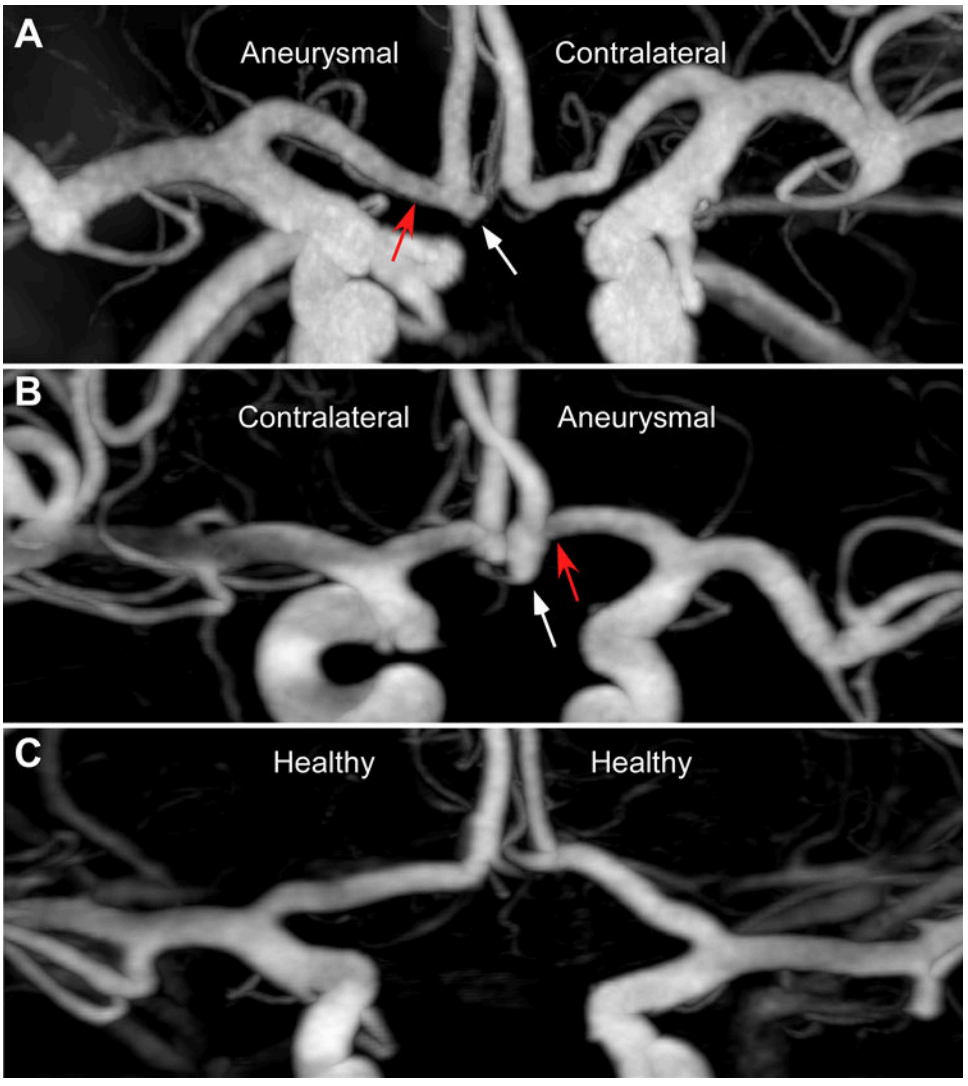


FIG. 2. A and B: Maximum intensity projection of bilateral 3DRA data for patients with unruptured ACoA aneurysms. *White arrows* indicate the site of the aneurysms, *red arrows* the locus of tapering. **C:** Maximum intensity projection of bilateral 3DRA data for a healthy control patient. Figure is available in color online only.

vessel WSS conditions of approximately 1.5 Pa at distal A_1 segments (one diameter from the ACoA bifurcation). Subsequently, steady flow was applied at the inlet of both models according to the resulting scaled velocity, with zero-gauge pressure at the outlets.

Postprocessing analysis was performed using EnSight (version 10.2, Ansys Inc.). The relative pressure (Fig. 4B) for the two models was evaluated through normalization by the pressure at the distal A_1 segment (distal planes in Fig. 4B). The WSS was evaluated for both models (Fig. 4C). Fluid velocity was evaluated along transversal planes through the ACoA bifurcation (Fig. 4D).

Results

Patient Demographics

The study included 48 unruptured ACoA aneurysms (32 females), 20 ruptured ACoA aneurysms (12 females), 37 nonaneurysmal contralateral sides corresponding to unruptured ACoA aneurysms (24 females), and 53 bilateral data sets from healthy control patients with no aneurysms (37 females). This resulted in a total of 211 angiographic 3D data sets available for analysis.

Univariate Statistical Analysis

This section describes tapering evaluation measured 1 mm from the ICA and ACoA bifurcations. Evaluations at 1.5 and 2 mm from bifurcations are consistent with these statistical results and are available in Supplementary Table 2.

Unruptured aneurysmal segments were compared with ruptured aneurysms, with their corresponding contralateral, and with the 3 healthy groups corresponding to dominant, nondominant, and codominant A_1 labeling (Table 1). There was no statistically significant age difference between patients with aneurysms and healthy patients for any of the groups studied.

Brought to you by Tufts University | Unauthenticated | Downloaded 11/04/25 02:23 PM UTC

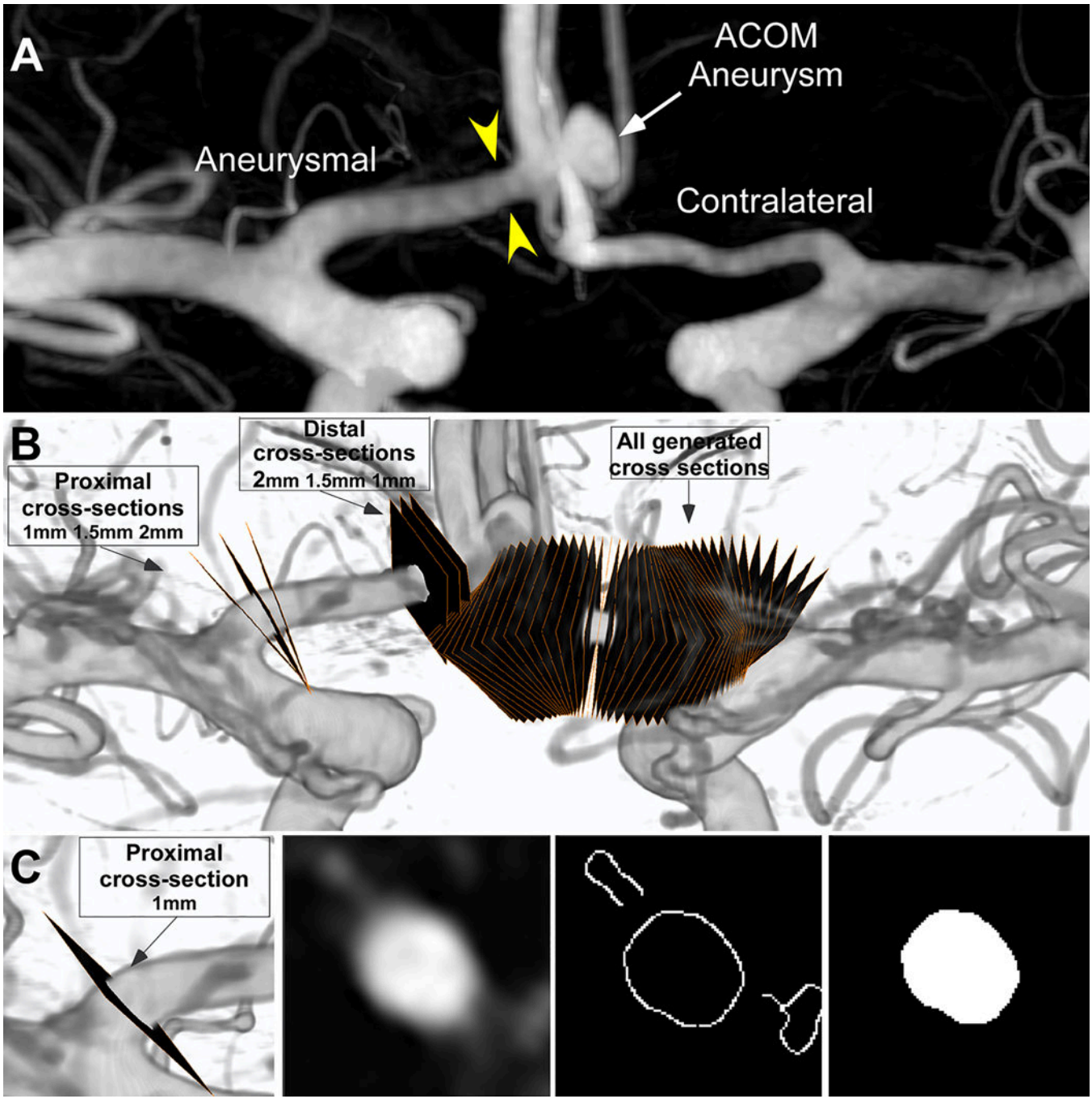


FIG. 3. A: Maximum intensity projection of bilateral 3DRA data for a patient with an unruptured ACoA aneurysm showing tapering (*arrows*). The aneurysmal A_1 (left/right) segment of the ACA was selected as the side that provided a complete filling of the aneurysm on the corresponding angiographic images. **B:** Cross-sectional cuts are automatically generated along the A_1 segments, and the distal and proximal cross-sections are selected at 1 mm. **C:** An edge detection filter is applied on each cross-sectional cut plane. This enables accurate and consistent measurements independent of user-applied brightness/contrast change. CSA of the A_1 segment is calculated based on the center of the detected A_1 edge. From left to right: 3D location of the cross-section, 2D cross-section through the 3D volume, edge detection applied to the 2D cross-section, identification of the CSA. Figure is available in color online only.

The sizes of the A_1 segments, as evaluated by distal CSA and proximal CSA, were similar between aneurysmal segments and dominant controls. As expected, aneurysmal A_1 segments had larger vessel calibers compared to codominant and nondominant controls, as well as nonaneurysmal contralaterals (Table 1). However, regardless of dominance label, healthy controls showed significantly less vessel tapering. Aneurysmal A_1 segments showed sig-

Brought to you by Tufts University | Unauthenticated | Downloaded 11/04/25 02:23 PM UTC

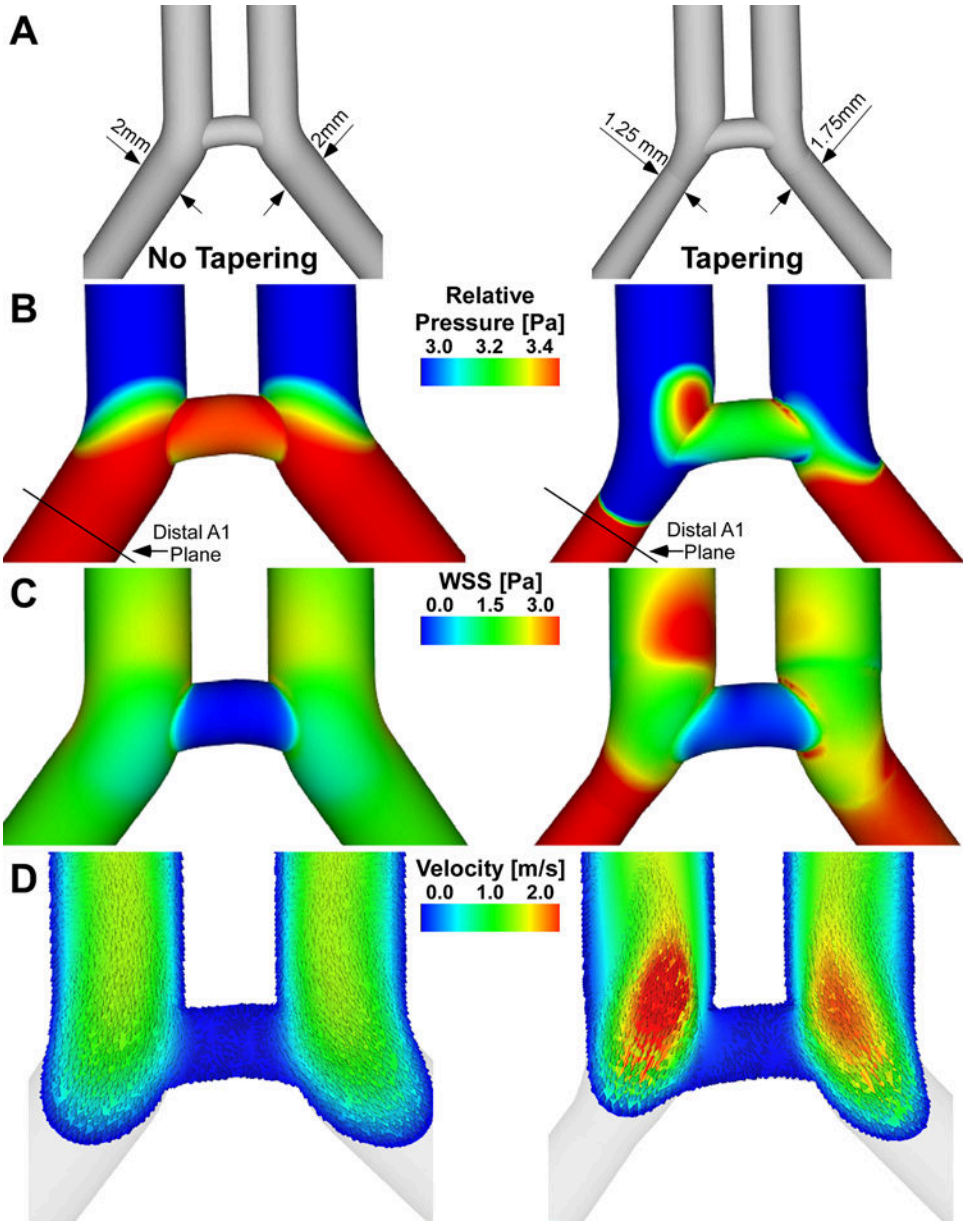


FIG. 4. A: Parametric models of the ACoA complex were created with (*right column*) and without (*left column*) tapering of the A_1 segments. **B:** Relative pressure was evaluated by normalizing local pressure to distal A_1 pressure, evaluated one diameter from the ACoA bifurcation. Tapering of the A_1 segment induces high relative pressure at the ACoA bifurcation, increasing with the degree of tapering. **C:** A_1 segment tapering induces high WSS on the corresponding A_2 segment wall, proximal to the ACoA bifurcation. **D:** A_1 segment tapering induces high flow velocity, increasing with the degree of tapering. Figure is available in color online only.

nificantly greater tapering with a lower tapering ratio compared to dominant (0.69 ± 0.13 vs 0.81 ± 0.16, p = 0.001), nondominant (0.69 ± 0.13 vs 0.87 ± 0.16, p < 0.0001), and codominant (0.69 ± 0.13 vs 0.82 ± 0.16, p < 0.0001) healthy controls (Table 1, Fig. 5). In fact, healthy controls showed a level of tapering similar to contralateral data sets. There was no statistically significant difference in tapering ratios between contralateral data sets and the 3 control groups (all healthy regardless of dominance labeling; 0.80 ± 0.17 vs 0.83 ± 0.16, p = 0.30). In addition, there was no statistically significant difference in A_1 tapering ratios between ruptured and unruptured aneurysms (0.69 ± 0.13 vs 0.64 ± 0.21, p = 0.26). Aneurysms occurred predominantly on dominant (79%) and codominant (17%) A_1 segments, with only 3 aneurysms occurring on nondominant A_1 segments.

Statistical evaluation after the exclusion of patients with acute SAH was consistent with the results presented above. Additional statistical evaluations using cross-section measurements at 1.5 mm and 2 mm from ICA and ACoA bifurcations were consistent with the results presented here. The additional data and analysis are available in Supplementary Table 2.

Brought to you by Tufts University | Unauthenticated | Downloaded 11/04/25 02:23 PM UTC

TABLE 1. Univariate statistical analysis of ACoA (A_1) parameters in discriminating between aneurysmal and control samples

Parameter	Unruptured Aneurysm (n = 48)	Ruptured Aneurysm (n = 20)	Contralateral Side (n = 37)	Healthy A_1 Segment		
				Dominant (n = 29)	Nondominant (n = 29)	Codominant (n = 48)
Distal CSA, mm^2						
Mean ± SD	4.05 ± 1.27	3.43 ± 1.16	2.49 ± 0.90	4.38 ± 1.17	2.50 ± 0.99	3.38 ± 1.07
p value		0.06	<0.0001*	0.21	<0.0001*	0.003*
Proximal CSA, mm^2						
Mean ± SD	5.97 ± 1.90	5.49 ± 1.55	3.18 ± 1.16	5.51 ± 1.14	2.90 ± 1.01	4.13 ± 0.98
p value		0.32	<0.0001*	0.14	<0.0001*	<0.0001*
Tapering ratio						
Mean ± SD	0.69 ± 0.13	0.64 ± 0.21	0.80 ± 0.17	0.81 ± 0.16	0.87 ± 0.16	0.82 ± 0.16
p value		0.26	0.001*	0.001*	<0.0001*	<0.0001*
A_1 length, mm						
Mean ± SD	14.71 ± 2.47	14.91 ± 2.28	15.33 ± 2.53	13.71 ± 1.88	14.74 ± 2.28	13.19 ± 1.72
p value		0.76	0.19	0.06	0.94	0.001*
Age, yrs						
Mean ± SD	57.77 ± 12.02	54.05 ± 11.56	56.74 ± 13.06	51.98 ± 13.78	51.98 ± 13.78	53.73 ± 13.06
p value		0.24	0.71	0.06	0.06	0.12
Females	32	12	24	15	15	22

The aneurysmal A_1 (left/right) segment was selected as the side that provided a complete filling of the aneurysm on the corresponding angiographic images. Healthy controls were evaluated based on flow and size as the dominant A_1 group (A_1 is 20% larger than the other A_1 segment), nondominant A_1 group (A_1 is 20% smaller than the other A_1 segment), and codominant A_1 group (the two A_1 segments have comparable sizes, within 20% difference). Distal CSA is the distal cross-sectional plane cut of the A_1 segment, 1 mm from the ACoA bifurcation. Proximal CSA is the proximal cross-sectional plane cut of the A_1 segment, 1 mm from the ICA bifurcation. Tapering ratio is the tapering of the A_1 segment, defined as distal CSA/proximal CSA. A_1 length is the length of the A_1 segment.

* Statistical significance ($p < 0.05$) relative to unruptured aneurysmal samples.

Matched-Pair Analysis

The A_1 segment was evaluated bilaterally on 37 unruptured ACoA aneurysms within the same patient and compared against the 37 corresponding contralateral sides (Table 2). In this subgroup, ACoA aneurysms occurred predominantly on dominant and codominant A_1 segments (35 samples, 95%).

Matched-pair statistical analysis showed that A_1 segments leading to aneurysmal ACoA bifurcation had significantly wider distal and proximal CSA compared to the corresponding contralateral (Fig. 5B and C), consistent with A_1 being the dominant side (Table 2). However, the aneurysmal A_1 had a significantly smaller tapering ratio corresponding to greater vessel tapering (0.68 ± 0.13 vs 0.80 ± 0.17, p = 0.0009) compared to the contralateral A_1 segment (Fig. 5A). A low tapering ratio corresponds to a more funnel type or firehose nozzle morphology of the vessel. Specifically, A_1 segments leading to aneurysms display greater vessel tapering progressing along the length of the segment. Bilaterally, the aneurysmal A_1 segment was significantly shorter compared to its corresponding contralateral (14.48 ± 2.30 vs 15.33 ± 2.53, p = 0.04). This is an important finding showing that tapering is not a function of the segment length.

To determine if vessel tapering is an attribute of dominant morphology rather than aneurysm presence, matched-pair statistical analysis was also evaluated in 29 healthy control pairs, between dominant and the corresponding nondominant contralateral. Similar to aneurysmal analysis, matched-pair statistical evaluation showed that the dominant healthy side had significantly wider distal and proximal CSA compared to the corresponding nondominant contralateral (Table 2). However, in contrast to aneurysm-bearing patients, the dominant A_1 segment in healthy patients showed a nonsignificant trend toward additional tapering compared to the nondominant side (0.81 ± 0.16 vs 0.87 ± 0.16, p = 0.07). It should be noted that, similar to aneurysmal samples, healthy dominant A_1 segments were also significantly shorter compared to their nondominant contralateral (13.71 ± 1.88 vs 14.74 ± 2.28, p = 0.008).

CFD Analysis

CFD analysis on the two parametric models showed that vessel tapering induces high relative pressure and high WSS at the ACoA bifurcation. The location of the focal high pressure and high WSS corresponds to the site where ACoA aneurysms are known to form in patients. Proximal vessel tapering induces high velocity at the ACoA bifurcation, a phenomenon not observed in the nontapered model. The greater the tapering of the A_1 segment, the more pronounced are these hemodynamic effects.

Discussion

ACoA aneurysms are the most commonly identified and ruptured aneurysms in the circle of Willis.[1] The anatomical variations of the anterior communicating complex, and the hemodynamic dependencies related to the vascular connection at the ACoA level, pose unique challenges for the morphological analysis of the related proximal (A_1 seg-

Brought to you by Tufts University | Unauthenticated | Downloaded 11/04/25 02:23 PM UTC

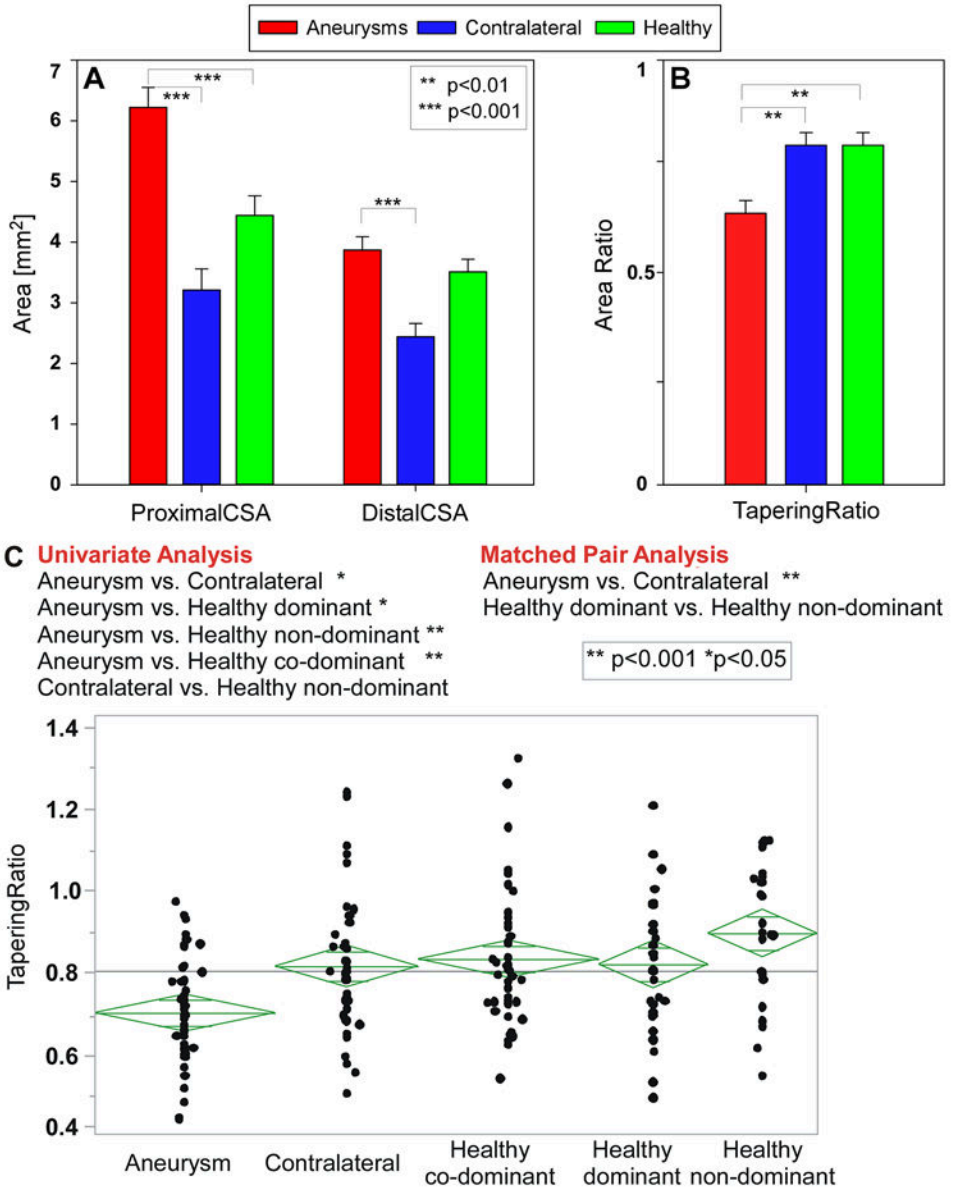


FIG. 5. A: Bar graph representation of differences in proximal and distal CSA between A_1 segments leading to aneurysmal, contralateral, and healthy data sets. **B:** Bar graph representation of differences in tapering ratio between A_1 segments leading to aneurysmal, contralateral, and healthy bifurcations. Dominant and codominant healthy samples are represented as one group. **C:** Distribution plots for the tapering ratio, and statistical comparison in univariate and matched-pair fashion for aneurysmal and control groups. A_1 segments leading to aneurysms had significantly greater tapering of the A_1 segment (lower tapering ratio). Figure is available in color online only.

TABLE 2. Matched-pair statistical analysis of ACoA (A_1) parameters between aneurysmal side and corresponding nonaneurysmal contralateral in patients with ACoA aneurysms, and between healthy patients in which contralateral A_1 segments are labeled as dominant and nondominant

Parameter	Aneurysm (n = 37)	Contralateral (n = 37)	p Value	Healthy Dominant (n = 29)	Healthy Nondominant (n = 29)	p Value
Distal CSA, mm^2	4.03 ± 1.26	2.49 ± 0.91	<0.001*	4.38 ± 1.17	2.50 ± 0.99	<0.001*
Proximal CSA, mm^2	6.00 ± 1.87	3.18 ± 1.16	<0.001*	5.51 ± 1.14	2.90 ± 1.01	<0.001*
Tapering ratio	0.68 ± 0.13	0.80 ± 0.17	0.0009*	0.81 ± 0.16	0.87 ± 0.16	0.07
A_1 length, mm	14.48 ± 2.30	15.33 ± 2.53	0.04*	13.71 ± 1.88	14.74 ± 2.28	0.008*

Data given as mean ± SD unless otherwise indicated.
* Statistical significance ($p < 0.05$) relative to unruptured aneurysmal samples.

Brought to you by Tufts University | Unauthenticated | Downloaded 11/04/25 02:23 PM UTC

ment) and distal (A_2 segment) vessels. In contrast to other cerebral bifurcations, such as the MCA or basilar artery, which are end vessels with a more treelike structure, the ACoA closes the circle of Willis and receives flow contributions from both A_1 segments, which cannot be studied in isolation. The characteristics of this location, and its high frequency of aneurysm formation, make the study of the ACA and communicating complex, and the understanding of the underlying mechanisms for ACoA aneurysm initiation and progression, particularly relevant.

Although cerebral aneurysm research tends to focus on the local morphological[8,9] and hemodynamic[9–12] characteristics of aneurysms, vessel morphology evaluation as it relates to aneurysm presence and rupture status is increasingly being evaluated as well. Lauric et al.[13] reported on the association between high vessel curvature and aneurysm presence. Baharoglu et al.[14] and Sadatomo et al.[15] showed the association between wide MCA bifurcation angle and occurrence of MCA aneurysms. Tütüncü et al.[16] confirmed the same wide-angle association at the basilar artery bifurcation. The caliber relationship between parent and daughter vessels was previously evaluated for the MCA segments,[6,17] and it was shown that, in contrast to healthy bifurcations, aneurysmal bifurcations deviate from the vascular optimality principle,[6] with daughter branches having larger calibers than the mother parent branch.

Lauric et al.[3] reported that M_1 segments leading to end-vessel MCA bifurcation aneurysms display a progressive narrowing, not observed in nonaneurysmal contralaterals or in healthy controls, which show no vessel tapering (tapering ratio = 1). This progressive tapering in aneurysmal models was shown to trigger high WSS and high positive WSS gradients at the bifurcation apex,[3,4] conditions previously associated with destructive endothelial remodeling consistent with aneurysmal initiation.[5] It should be noted that this progressive tapering is distinct from the pronounced and more sudden atherosclerotic stenosis previously reported in Japanese patients,[4] although both lead to similar flow acceleration and to the hemodynamic "firehose nozzle effect."

This study evaluated the tapering of the A_1 segment of the ACA in bilateral fashion on unruptured ACoA aneurysms (without risk of vasospasm, which could be confounding had we chosen ruptured cases), on the corresponding contralateral side, and on healthy controls from patients without any intracranial aneurysms. Ruptured and unruptured aneurysms were evaluated as separate groups to remove the effect of possible vasospasm on the overall statistical analysis. The comparison with the contralateral side was performed as matched-pair analysis, in which each patient acted as his or her own control, without any dependencies on age, health, or environmental characteristics. Healthy controls were evaluated as A_1 dominant, nondominant, and codominant groups, to control for the vessel vascular role within the anterior communication complex. Even under these strict conditions, our results show that, similar to reports on MCA bifurcations, the A_1 segments leading to ACoA aneurysms had significantly greater vessel tapering compared to contralateral and healthy controls. Importantly, there was no statistically significant tapering difference between dominant and nondominant healthy controls. This suggests that the greater vessel tapering is associated with ipsilateral downstream aneurysm presence and is not just a function of vascular dominance. In addition, whereas the tapering was more pronounced on the dominant side, this vessel length was significantly shorter compared to the contralateral nondominant side, showing that the tapering is not a consequence of progressive tapering over the length of the vessel. This was also evident in healthy patients, in which the dominant side was significantly shorter than the nondominant contralateral ($p = 0.008$), but there was not a statistically significant tapering difference. These results suggest that vessel dominance is associated with a shorter A_1 segment and overall greater tapering compared to the nondominant side, significantly more so in the presence of aneurysms. Hemodynamically, in our CFD modeling, tapering of the A_1 segment was associated with distal high relative pressure, high WSS, and high velocity at the ACoA bifurcation, and this hemodynamic effect increased with the degree of tapering.

These results show that the tapering phenomenon first associated with MCA aneurysms[3] is not limited to that particular location or to just end-vessel bifurcations, and is now generalized to communicating vessel bifurcation ACoA aneurysms. Although a local condition on the cerebral vasculature, vessel tapering and the associated firehose nozzle effect appear to be related to aneurysm presence at vascular bifurcations, independent of aneurysm location. These results raise the possibility that similar findings would be true for other bifurcation segments such as the basilar artery and the proximal internal carotid artery bifurcation. Future studies will be required to verify this hypothesis and confirm a generalized role of tapering effect in vasculature prone to aneurysm formation.

It should be noted that there are, however, some ACA location-specific characteristic differences. In contrast to the MCA M_1 segment, the healthy and contralateral ACoA groups did show some baseline vessel tapering (tapering ratio < 1). This phenomenon was not detected in MCA M_1 segments, where both healthy and contralateral samples had a tapering ratio of 1. This finding requires future evaluation, but it may possibly be related to the relative hemodynamic demand of perforating vessels (recurrent artery of Heubner) branching off the A_1 segment and lenticulostriate arteries off the M_1 segment.

Future research is needed to determine the mechanistic basis of this tapering phenomenon, whether it is structural or contractile, reversible, or permanent, and if it is related to gender and/or predisposing risk factors such as smoking, polycystic kidney disease,[18] or connective tissue anomalies. It should be noted that, similar to observations on M_1 segments,[3] A_1 tapering seems to be a gradual effect with no areas of focal stenosis such as those reported in Japanese populations.[4] Still, it remains to be investigated if this is a structural phenomenon, possibly related to arteriosclerosis, which precedes and promotes aneurysm formation, or if it is a protective response, manifesting as focal vasoconstriction, which may be responsive to vasodilator agents.

Our results expand the contribution of vessel tapering in the presence of aneurysms, as a more generalizable and universal finding, affecting more than 50% of cerebral aneurysmal lesions. Longitudinal follow-up studies would

Brought to you by Tufts University | Unauthenticated | Downloaded 11/04/25 02:23 PM UTC

also be of interest in defining the temporal contribution to aneurysm initiation and development. The apparent prevalence of this tapering phenomenon warrants future analysis that should provide insight into clinical relevance, methods for morphological screening of cerebral bifurcations, and potential therapeutic strategies. Although not yet investigated, it should be noted that favorable tapering remodeling is a likely effect of stent-mediated coiling, similar to the angular remodeling previously reported[18] in which stent placement at bifurcations led to a significant biphasic angular modification, effectively altering the bifurcation morphology.[19] We hypothesize that stent coiling is similarly reducing the extent of vessel tapering, further mitigating conditions for aneurysm origination. In addition, the question arises as to whether this persistent vascular constriction represented by vessel tapering responds to either vasodilators or to smooth muscle relaxants as potential therapeutic approaches. Conversely, other risk factors such as smoking may increase blood flow velocity, possibly via vasoconstriction, as suggested by Boyajian et al.[20] and Kochanowicz et al.[21] The clinical implication of our findings for lowering the risk for aneurysm initiation and recurrence requires further research.

Study Limitations

This research showed that quantitative analysis of caliber variations along the A_1 segment of the ACA can be used to discriminate between aneurysmal and nonaneurysmal ACoA bifurcations. As with similar retrospective research, the association between vessel tapering and the impact of the described "firehose nozzle effect" on aneurysm presence suggests a correlation but does not imply causation. The conclusions of this study will require validation by further prospective research to confirm the hypothetical role of parent vessel tapering.

An additional question involves whether the narrowing effect demonstrated here represents an imaging artifact due to flow effects related to aneurysm presence. We believe this is unlikely given the relatively small sizes of the aneurysms in this population and the fact that controls also displayed some degree of caliber tapering. In addition, the fact that the same phenomenon was seen in the MCA, which is laterally directed and less central than the ACoA, and for which any imaging artifact would be in the reverse direction, further argues against this possibility. It should be noted that the use of CSA is more sensitive to caliber change when compared to diameter change. For instance, a tapering ratio of 0.67 indicates a 33% decrease in CSA compared to a 19% decrease in diameter (assuming a circular CSA). This sensitivity, combined with high-resolution rotational angiography and the critical 3D edge detection filter, allowed for the identification of intensity and contrast-insensitive subtle changes in vessel size.

Conclusions

In contrast to healthy controls, A_1 segments leading to ACoA aneurysms demonstrate significant progressive distal tapering, which was previously associated with aneurysmogenic hemodynamic conditions at the bifurcation apex akin to flow acceleration seen in a firehose nozzle. These results are consistent with those previously reported for MCA bifurcation aneurysms and extend this phenomenon from end-type to communicating-type vascular bifurcations. These results warrant further analysis into clinical relevance and implications, methods for morphological screening of cerebral bifurcations, and potential therapeutic strategies.

References

1. Sekhar LN, Natarajan SK, Britz GW, Ghodke B. Microsurgical management of anterior communicating artery aneurysms. *Neurosurgery*. 2007;61(5)(suppl 2):273-292.
2. International Study of Unruptured Intracranial Aneurysms Investigators. Unruptured intracranial aneurysms—risk of rupture and risks of surgical intervention. *N Engl J Med*. 1998;339(24):1725-1733.
3. Lauric A, Greim-Kuczewski K, Antonov A, et al. Proximal parent vessel tapering is associated with aneurysm at the middle cerebral artery bifurcation. *Neurosurgery*. 2019;84(5):1082-1089.
4. Antonov A, Kono K, Greim-Kuczewski K, Hippelheuser JE, Lauric A, Malek AM. Proximal stenosis is associated with rupture status in middle cerebral artery aneurysms. *World Neurosurg*. 2018;109:e835-e844.
5. Meng H, Swartz DD, Wang Z, Hoi Y, Kolega J, et al. A model system for mapping vascular responses to complex hemodynamics at arterial bifurcations in vivo. *Neurosurgery*. 2006;59(5):1094-1101.
6. Baharoglu MI, Lauric A, Wu C, Hippelheuser J, Malek AM. Deviation from optimal vascular caliber control at middle cerebral artery bifurcations harboring aneurysms. *J Biomech*. 2014;47(13):3318-3324.
7. Schirmer CM, Malek AM. Wall shear stress gradient analysis within an idealized stenosis using non-Newtonian flow. *Neurosurgery*. 2007;61(4):853-864.
8. Baharoglu MI, Lauric A, Gao BL, Malek AM. Identification of a dichotomy in morphological predictors of rupture status between sidewall- and bifurcation-type intracranial aneurysms. *J Neurosurg*. 2012;116(4):871-881.
9. Xiang J, Natarajan SK, Tremmel M, Ma D, Mocco J, et al. Hemodynamic-morphologic discriminants for intracranial aneurysm rupture. *Stroke*. 2011;42(1):144-152.
10. Lauric A, Hippelheuser J, Cohen AD, Kadasi LM, Malek AM. Wall shear stress association with rupture status in volume matched sidewall aneurysms. *J Neurointerv Surg*. 2014;6(6):466-473.
11. Jou LD, Lee DH, Morsi H, Mawad ME. Wall shear stress on ruptured and unruptured intracranial aneurysms at the internal carotid artery. *AJNR Am J Neuroradiol*. 2008;29(9):1761-1767.
12. Miura Y, Ishida F, Umeda Y, Tanemura H, Suzuki H, et al. Low wall shear stress is independently associated with the rupture status of middle cerebral artery aneurysms. *Stroke*. 2013;44(2):519-521.
13. Lauric A, Safain MG, Hippelheuser J, Malek AM. High curvature of the internal carotid artery is associated with the presence of intracranial aneurysms. *J Neurointerv Surg*. 2014;6(10):733-739.
14. Baharoglu MI, Lauric A, Safain MG, Hippelheuser J, Wu C, Malek AM. Widening and high inclination of the middle cerebral artery bifurcation are associated with presence of aneurysms. *Stroke*. 2014;45(9):2649-2655.
15. Sadatomo T, Yuki K, Migita K, Imada Y, Kuwabara M, Kurisu K. Differences between middle cerebral artery bifurcations with normal anatomy and those with aneurysms. *Neurosurg Rev*. 2013;36(3):437-445.
16. Tütüncü F, Schimansky S, Baharoglu MI, Gao B, Calnan D, et al. Widening of the basilar bifurcation angle: association

Brought to you by Tufts University | Unauthenticated | Downloaded 11/04/25 02:23 PM UTC

with presence of intracranial aneurysm, age, and female sex. *J Neurosurg*. 2014;121(6):1401-1410.
17. Sadatomo T, Yuki K, Migita K, Taniguchi E, Kodama Y, Kurisu K. Morphological differences between ruptured and unruptured cases in middle cerebral artery aneurysms. *Neurosurgery*. 2008;62(3):602-609.
18. Gao B, Baharoglu MI, Cohen AD, Malek AM. Stent-assisted coiling of intracranial bifurcation aneurysms leads to immediate and delayed intracranial vascular angle remodeling. *AJNR Am J Neuroradiol*. 2012;33(4):649-654.
19. Gao B, Baharoglu MI, Cohen AD, Malek AM. Y-stent coiling of basilar bifurcation aneurysms induces a dynamic angular vascular remodeling with alteration of the apical wall shear stress pattern. *Neurosurgery*. 2013;72(4):617-629.
20. Boyajian RA, Otis SM. Acute effects of smoking on human cerebral blood flow: a transcranial Doppler ultrasonography study. *J Neuroimaging*. 2000;10(4):204-208.
21. Kochanowicz J, Lewko J, Rutkowski R, Turek G, Sieskiewicz A, et al. Influence of smoking cigarettes on cerebral blood flow parameters. *Biol Res Nurs*. 2015;17(1):8-12.

Disclosures

The authors report no conflict of interest concerning the materials or methods used in this study or the findings specified in this paper.

Author Contributions

Conception and design: Malek. Acquisition of data: all authors. Analysis and interpretation of data: Malek, Silveira, Lesha, Breton. Drafting the article: Lauric. Critically revising the article: Malek. Reviewed submitted version of manuscript: Malek. Approved the final version of the manuscript on behalf of all authors: Malek. Statistical analysis: Malek, Lauric.

Supplemental Information

Online-Only Content

Supplemental material is available with the online version of the article.

Supplementary Figure and Tables. https://thejns.org/doi/suppl/10.3171/2021.5.JNS204389.

Correspondence

Adel M. Malek: Tufts Medical Center, Boston, MA. amalek@tuftsmedicalcenter.org.

Brought to you by Tufts University | Unauthenticated | Downloaded 11/04/25 02:23 PM UTC